Science AAAS

The Unusual Nature of Recent Snowpack Declines in the North American Cordillera

Gregory T. Pederson, *et al.*

Science **333**, 332 (2011);
DOI: 10.1126/science.1201570

This copy is for your personal, non-commercial use only.

If you wish to distribute this article to others, you can order high-quality copies for your colleagues, clients, or customers by clicking here.

Permission to republish or repurpose articles or portions of articles can be obtained by following the guidelines here.

The following resources related to this article are available online at www.sciencemag.org (this infomation is current as of July 18, 2011):

Updated information and services, including high-resolution figures, can be found in the online version of this article at:
http://www.sciencemag.org/content/333/6040/332.full.html

Supporting Online Material can be found at:
http://www.sciencemag.org/content/suppl/2011/06/08/science.1201570.DC1.html

This article **cites 35 articles**, 6 of which can be accessed free:
http://www.sciencemag.org/content/333/6040/332.full.html#ref-list-1

This article appears in the following **subject collections:**
Geochemistry, Geophysics
http://www.sciencemag.org/cgi/collection/geochem_phys

Downloaded from www.sciencemag.org on July 18, 2011

Science (print ISSN 0036-8075; online ISSN 1095-9203) is published weekly, except the last week in December, by the American Association for the Advancement of Science, 1200 New York Avenue NW, Washington, DC 20005. Copyright 2011 by the American Association for the Advancement of Science; all rights reserved. The title *Science* is a registered trademark of AAAS.

27. A. Saito, H. C. Foley, *Microporous Mater.* **3**, 543 (1995).
28. E. L. Wu, S. L. Lawton, D. H. Olson, A. C. Rohrman Jr., G. T. Kokotailo, *J. Phys. Chem.* **83**, 2777 (1979).
29. R. Ryoo, S. H. Joo, S. Jun, *J. Phys. Chem. B* **103**, 7743 (1999).
30. J. B. Higgins *et al.*, *Zeolites* **8**, 446 (1988).
31. A. Corma *et al.*, *Chem. Mater.* **20**, 3218 (2008).
32. J. H. Lunsford, W. P. Rothwell, W. Shen, *J. Am. Chem. Soc.* **107**, 1540 (1985).
33. Q. Zhao *et al.*, *J. Phys. Chem. B* **106**, 4462 (2002).

Acknowledgments: This work was supported by the National Honor Scientist Program (20100029665) and World Class University Program (R31-2010-000-10071-0) of the Ministry of Education, Science and Technology in Korea. The work at UCSB was supported by the U.S. NSF under grant CHE-0924654 and the U.S. Department of Energy through the Institute of Multiscale Materials Studies at Los Alamos National Laboratory and Basic Energy Sciences grant DE-FG02-03ER15467. R.J.M. is grateful to the Warren and Katharine Schlinger Foundation for a doctoral research fellowship. Solid-state NMR measurements were conducted using the Central Facilities of the NSF-supported UCSB Material Research Laboratory through grant DMR-05-20415. A patent has been filed by KAIST that claims new materials, preparation method, and catalytic applications thereof [10-2010-0064200, Korea, and PCT/KR2011/004128, Patent Cooperation Treaty (PCT)]. Author contributions: R.R. planned and supervised the project; K.N and R.R. wrote the manuscript; K.N., C.J., J.K., and J.J. synthesized surfactants and porous materials and performed XRD, SEM, and adsorption; K.N. performed catalytic investigations; K.C. performed TEM investigations; Y.S. analyzed acidity with ^{31}P NMR; and R.J.M. and B.F.C. performed 2D NMR investigations. B.F.C. (bradc@engineering.ucsb.edu) was responsible for the 2D NMR part. The authors declare that there are no competing financial interests. R.R., K.N., C.J., J.K., and J.J. are applicants for a patent related to this work. The patent deals with an invention of new materials and their synthesis method and applications. The patent was submitted to Korea on 5 July 2010 with application no. 10-2010-0064200 and submitted to PCT on 7 June 2011 with application no. PCT/KR2011/004128.

Supporting Online Material
www.sciencemag.org/cgi/content/full/333/6040/328/DC1
Materials and Methods
SOM Text
Figs. S1 to S17
Tables S1 and S2
References (*34*–*38*)

17 February 2011; accepted 20 May 2011
10.1126/science.1204452

The Unusual Nature of Recent Snowpack Declines in the North American Cordillera

Gregory T. Pederson,[1,2,3]* Stephen T. Gray,[3,4] Connie A. Woodhouse,[3,5] Julio L. Betancourt,[6] Daniel B. Fagre,[1] Jeremy S. Littell,[7] Emma Watson,[8] Brian H. Luckman,[8] Lisa J. Graumlich[9]

In western North America, snowpack has declined in recent decades, and further losses are projected through the 21st century. Here, we evaluate the uniqueness of recent declines using snowpack reconstructions from 66 tree-ring chronologies in key runoff-generating areas of the Colorado, Columbia, and Missouri River drainages. Over the past millennium, late 20th century snowpack reductions are almost unprecedented in magnitude across the northern Rocky Mountains and in their north-south synchrony across the cordillera. Both the snowpack declines and their synchrony result from unparalleled springtime warming that is due to positive reinforcement of the anthropogenic warming by decadal variability. The increasing role of warming on large-scale snowpack variability and trends foreshadows fundamental impacts on streamflow and water supplies across the western United States.

In the mountains of western North America, snowpack controls the amount of runoff (*1*, *2*), affects temperature through surface albedo feedbacks (*3*, *4*), and influences myriad ecosystem processes (*5*–*8*). In much of this region, snowpack declined since the 1950s (*2*, *9*–*11*), and continued reductions are expected throughout the 21st century and beyond (*2*, *12*). When coupled with increasing demand, additional warming-induced snowpack declines would threaten many current water storage and allocation strategies (*13*) and lead to substantial strain on related infrastructure and overall supplies. Climate model simulations shed light on the relationships between greenhouse gas forcing and observed shifts in regional temperatures and hydrology (*2*), but longer-duration records are needed to characterize the range of natural snowpack variability, particularly at decadal-to-multidecadal time scales (*14*). Did declines similar in duration, magnitude, and extent occur over the past ~1000 years, or are the recent snowpack losses unprecedented? How were previous snowpack declines driven by known mechanisms of temperature and precipitation variability, and to what degree can decadal-to-multidecadal climate variability amplify or dampen future warming-induced trends?

To address these questions, we developed annually resolved, multi-century to millennial-length (500- to >1000-year) snowpack reconstructions for the headwaters of the Columbia, Missouri, and Colorado Rivers. Collectively, these basins serve as the primary water source for >70 million people, and 60 to 80% of their water originates as snowpack (*1*, *2*). Reconstructions are based on an extensive network of tree-ring sites and provide information on patterns and processes across spatial and temporal scales relevant to water- and natural-resource management (Fig. 1).

Tree rings have long been used to reconstruct precipitation, drought (*15*, *16*), streamflow (*17*, *18*), and temperature (*19*, *20*), but to date there has been no systematic effort to produce multi-scale snowpack reconstructions for all three of these river basins. Previous studies in the region show that in certain topographic, edaphic, and climatic settings, the amount of water available to trees during the growing season is largely controlled by the amount of water in the antecedent snowpack (*18*, *21*). We capitalized on these snow-water-growth linkages by using existing tree-ring collections from areas where precipitation is dominated by snowfall and by sampling trees known to be sensitive to snowpack (*18*, *21*). To further isolate the snowpack signal, particularly in the northern portions of the study area, we used recently collected tree-ring records from species whose seasonal biology (timing of tree-ring growth) ties them closely to snow (*22*, *23*).

For calibration of the tree-ring–based reconstructions, continuous annual, sub-watershed (roughly 40,000 ± σ 25,000 km^2) snowpack data sets were constructed by standardizing individual 1 April snow water equivalent (SWE) records to unit deviation then averaging across all records from each watershed (fig. S1 and table S1) (*24*). Snowpack as measured on 1 April is a crucial component of regional runoff forecasting and water supply evaluations, and records of 1 April SWE are generally longer than for any other time of the year. In addition, 1 April measurements often approximate maximum SWE accumulation in our study watersheds (*4*, *11*), although peak accumulation timing can vary substantially at individual measurement sites. Elevations of individual measurement sites in the Upper Colorado subregion (Fig. 1) tend to be higher than those in the Greater Yellowstone (2807 ± σ 311 m versus 2307 ± σ 291 m), and sites in the Greater Yellowstone region are higher on average than those in the Northern Rockies (~1550 ± σ 424 m). Overall, the 27 composite snowpack reconstructions

[1]U.S. Geological Survey (USGS), Northern Rocky Mountain Science Center, 2327 University Way, Suite 2, Bozeman, MT 59715, USA. [2]School of Natural Resources, University of Arizona, 325 Biosciences East, Tucson, AZ 85721, USA. [3]Laboratory of Tree-Ring Research, University of Arizona, 105 West Stadium, Tucson, AZ 85721, USA. [4]Department of Civil and Architectural Engineering, University of Wyoming, Laramie, WY 82071, USA. [5]School of Geography and Development, 412 Harvill Building, University of Arizona, Tucson, AZ 85721–0076, USA. [6]USGS, National Research Program, Water Resources Division, Tucson, AZ 85719, USA. [7]Climate Impacts Group, University of Washington, Post Office Box 355672, Seattle, WA 98195–5672, USA. [8]Department of Geography, University of Western Ontario, London, Ontario N6A 5C2, Canada. [9]College of the Environment, University of Washington, Post Office Box 355679, Seattle, WA 98195–5679, USA.

*To whom correspondence should be addressed. E-mail: gpederson@usgs.gov

Downloaded from www.sciencemag.org on July 18, 2011

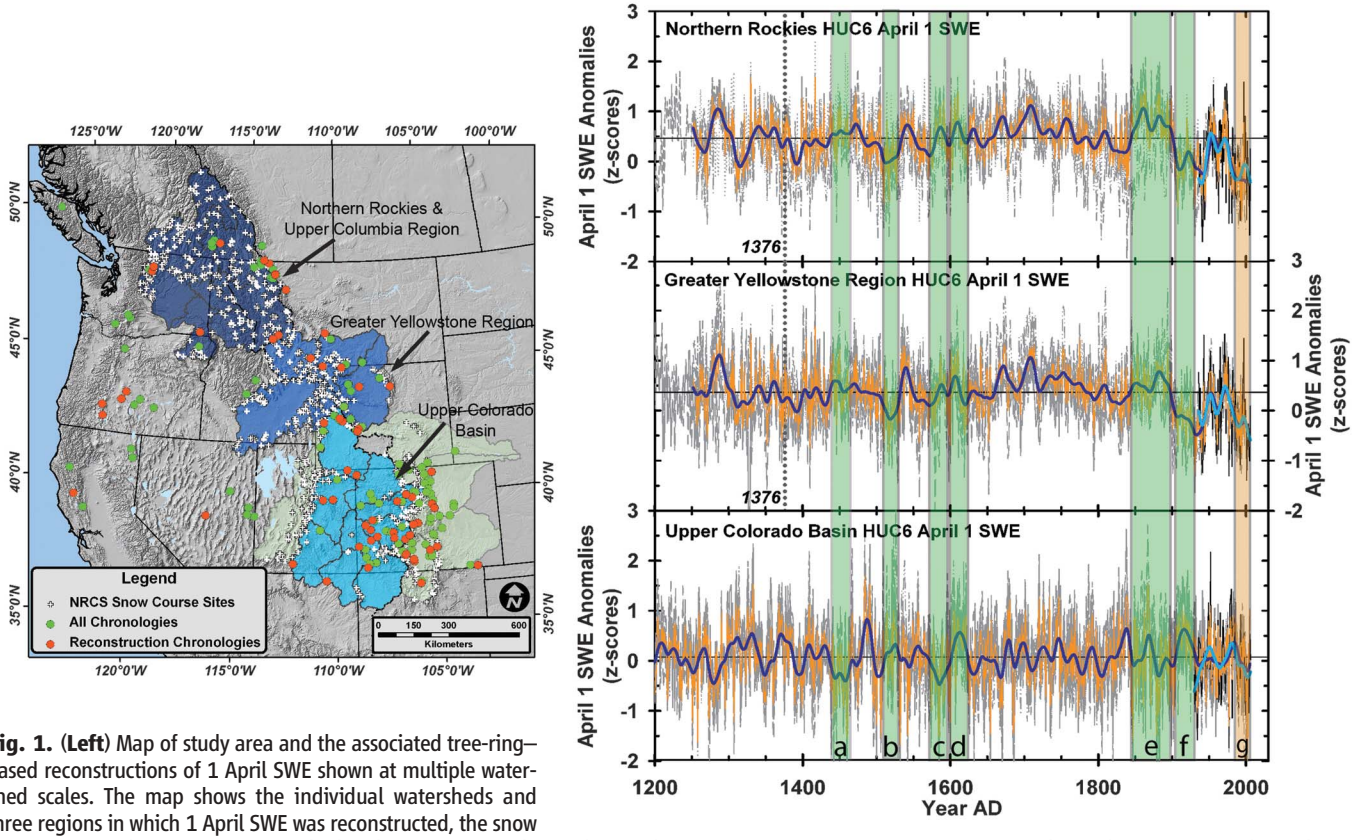

Fig. 1. (**Left**) Map of study area and the associated tree-ring–based reconstructions of 1 April SWE shown at multiple watershed scales. The map shows the individual watersheds and three regions in which 1 April SWE was reconstructed, the snow course sites used to generate watershed-scale averages of observed 1 April SWE, the full set of potential predictor chronologies (green circles), and the final set of chronologies that entered into one or more SWE reconstruction models as a predictor (orange circles). (**Right**) The graphs of the 1 April SWE reconstructions show the individual watershed reconstructions of 1 April SWE (gray lines) by region and latitude, the regional SWE average calculated from each individual reconstruction (orange line), and a 20-year cubic-smoothing spline (50% frequency cutoff) of the regional SWE average (dark blue line). For the Northern Rockies and Greater Yellowstone region, a cut-off date of 1376 is shown (dotted vertical line) because of decreasing sample depth and increasing reconstruction uncertainty. The 20th century records of observed 1 April SWE are plotted for each large region (black lines) and smoothed with a 20-year cubic-smoothing spline to highlight decadal-scale variability (light blue line) coherent with the snowpack reconstructions. Shaded intervals show decadal-scale SWE anomalies mapped in Figs. 2 and 4. Lettering corresponds to the mapped intervals. The observed and reconstructed SWE records are plotted as anomalies from the long-term average, which was calculated by using 1400 to 1950 C.E. as a base period. Other base periods were used to calculate the long-term average SWE conditions, yielding highly similar estimates (table S6).

skillfully capture interannual to multidecadal variability in observed 1 April SWE records (figs. S1 and S2 and tables S2 to S5) and provide detailed estimates of long-term snowpack history (*24*).

The 1 April SWE reconstructions (Fig. 1) show that for the northern cordillera—collectively the Greater Yellowstone and Northern Rocky Mountain subregions that encompass the headwaters of the Columbia and Missouri River drainages—there were only two periods (~1300 to 1330 C.E. and 1511 to 1530 C.E.) of sustained low snowpack in the past 800 years that are comparable with the early and late 20th century (~1900 to 1942 C.E. and ~1980 to present). In contrast, generally high snowpack conditions prevailed across the northern cordillera from the 1650s to the 1890s, coinciding with the maximum Holocene advance of glaciers (*25*) and a period of reduced fire activity across the West (*26*). In particular, two notable, decadal-scale high snowpack anomalies in the northern cordillera (~1695 to 1735 C.E. and 1845 to 1895 C.E.) coincided with cool summer temperatures (*19*) and with major intervals of Little Ice Age (LIA) glacier advance (Figs. 1E and 2E) (*25*). A paucity of positive decadal-scale snowpack anomalies in the southern cordillera—roughly the Upper Colorado headwaters (Figs. 1, 2E, and 3)—in conjunction with warmer summer temperatures (*20*) may explain the lack of a substantial LIA glacial advance over that subregion.

Snowpack reconstructions across the entire latitudinal gradient show pronounced interannual to multidecadal variability (fig. S2), but with distinct regional modes marked by a north-south (N-S) dipole [Figs. 2 and 3 and supporting online material (SOM) text]. The Greater Yellowstone and Northern Rocky Mountain watersheds exhibit decadal-scale and longer-term phasing of snowpack anomalies that are typically opposite those within the Upper Colorado. For example, the periods from roughly 1440 to 1470 C.E. (Figs. 1A and 2A) and 1550 to 1600 C.E. (Figs. 1C and 2C) (*15*, *16*) featured sustained low snowpack conditions centered over the Upper Colorado. During the same intervals, northern cordillera watersheds generally experienced average to above-average snowpack. In contrast, severe low snowpack conditions across the northern cordillera prevailed from 1511 to 1530 C.E., whereas the Upper Colorado experienced average to high snowpack (Figs. 1B and 2B). Comparison of the full multicentury reconstructions for all three regions shows that this antiphasing is generally robust through time (Fig. 3 and SOM text).

The N-S dipole suggests that sustained departures in the average latitudinal position of wintertime stormtracks are responsible for persistent snowpack anomalies. This is consistent with forcing related to interannual [El Niño–Southern Oscillation (ENSO)] and decadal [Pacific Decadal Oscillation (PDO)] sea surface–temperature (SST) variability in the Pacific Ocean, which tends to shift cool season storm tracks north-to-south across western North America (*4*, *27*). Specifically, when the tropical Pacific and northeast Pacific are warm the Pacific Northwest/northern Rockies are dry, southwestern North America is wet, and vice versa (*27*–*29*). Observed early to mid-20th century declines (~1900 to 1942 C.E.) in snowpack

Downloaded from www.sciencemag.org on July 18, 2011

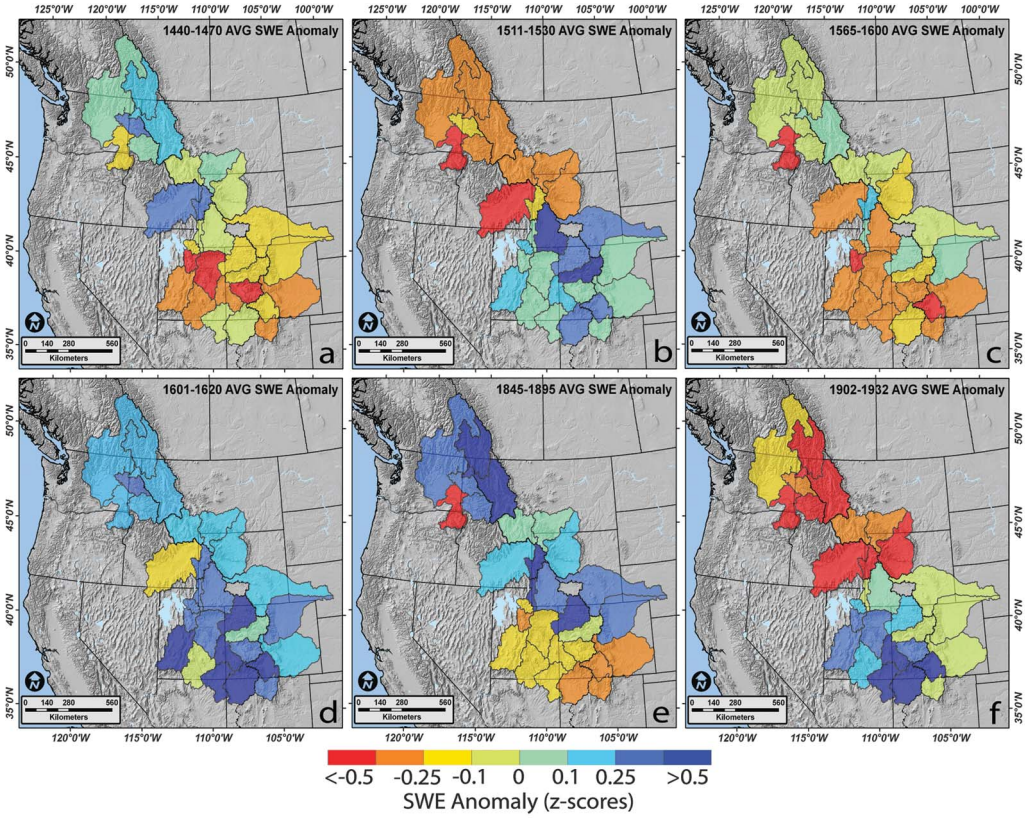

Fig. 2. Decadal departures in reconstructed 1 April SWE for watersheds predominately within the U.S. portion of the North American cordillera. Maps show average SWE conditions over the following intervals previously highlighted in Fig. 1: (**A**) 1440 to 1470, (**B**) 1511 to 1530, (**C**) 1565 to 1600, (**D**) 1601 to 1620, (**E**) 1845 to 1895, and (**F**) 1902 to 1932. The mapped SWE anomalies were calculated by averaging annual conditions for each hydrologic unit code (HUC) 6 watershed over the time interval shown and are plotted as anomalies from the long-term regional mean (1400 to 1950 AD). The final data sets along with the ability to generate user-defined maps of interannual- to interdecadal-scale departures in reconstructed and observed SWE are provided at www.nrmsc.usgs.gov/NorthAmerSnowpack/.

across the northern cordillera (Figs. 1F and 2F) coincided with warm SSTs across the Gulf of Alaska (positive PDO) (*30*), which resulted in pronounced meridional flows and a southerly stormtrack that delivered anomalously high winter precipitation to the Upper Colorado Basin. In the case of the Upper Colorado, this yielded a relative lack of drought and high river flows (*17*, *18*).

Although Pacific Basin forcing of precipitation and the resulting N-S dipole have been defining features of snowpack variability for the past millennium, several notable exceptions do occur. Cordillera-wide periods of low snowpack shown for the 1350s, 1400s, and post-1980s era (Fig. 3) correspond with times of anomalous warmth at regional and hemispheric scales (*19*, *20*, *31*), suggesting that temperature could be a direct or indirect control on snowpack anomalies of the same sign across the entire cordillera (*31*). Likewise, cool temperatures in the early 17th century (~1600 to 1620 C.E.) coincided with high snowpack conditions across the North American cordillera (Figs. 1D and 3). Interannual to decadal modes of ocean-atmosphere variability (related to ENSO and PDO) also may influence subcontinental-scale warming or cooling from February to May, which are the critical months for snow accumulation and melt in western North America (*1*, *2*, *9*, *14*, *32*). West-wide spring warming since ~1976 to 1984, coincident with warming in the tropical and northeast Pacific and anomalously high geopotential heights over western North America, has increased freezing levels, reduced snow accumulation, and

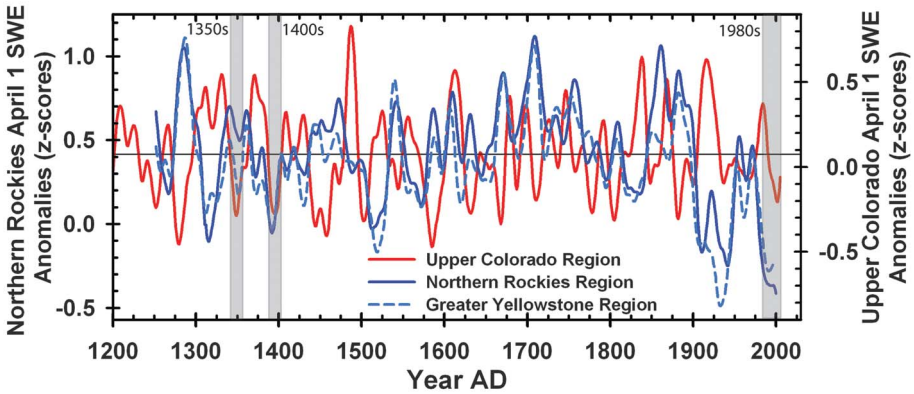

Fig. 3. Decadal-scale antiphasing of the N-S snowpack dipole and periods of synchronous snowpack decline. The 20-year splines of the regional average snowpack anomalies highlight antiphasing and variability at decadal scales. The shaded bars highlight periods of synchronous snowpack decline.

advanced the onset of snowmelt and green-up (*9*, *14*, *32*).

Previous work that used both observations and simulations suggests that temperature is especially important for driving snowpack dynamics in the Northern Rockies (*1*, *2*, *4*, *9*–*11*). The Northern Rockies are relatively low in elevation and snow mass; winters and springs at snow-monitoring sites are ~3°C warmer than in the Upper Colorado River subregion (fig. S3). In the Northern Rockies, the sensitivity to temperature fluctuations is evident in the anomalously high snowpack and glacial advance during the LIA as well as in anomalously low snowpack throughout most of the 20th century. On the other hand, the higher and cooler elevations of the southern cordillera probably buffered the snowpack from substantial temperature-driven losses, at least to date. Taken as a whole, evidence is mounting that projected warming could push mean winter temperatures at most snow-monitoring sites in the Northern Rockies past the 0°C isotherm and the entire snow-accumulation zone past the 0°C isotherm in April (fig. S3).

In the Upper Colorado watersheds, snowpack reconstructions can also be compared against existing long-term records of streamflow variability (*17*, *18*). Periods of high snowpack generally coincide with high flows and vice versa (fig. S4). There are times, however, when regional warming

Downloaded from www.sciencemag.org on July 18, 2011

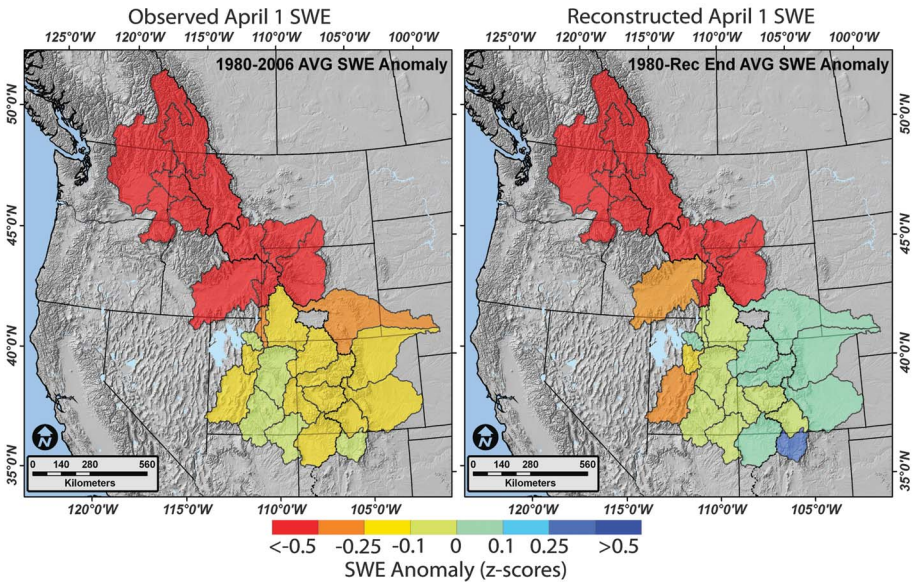

Fig. 4. Post-1980 average 1 April SWE conditions. Maps of post-1980 average SWE conditions (Fig. 1G) are plotted as anomalies from the regional long-term mean (1400 to 1950 C.E.) for the (**left**) observational record and (**right**) tree-ring–based reconstructions. The map showing average reconstructed SWE values is not exactly equivalent to the observational record because many individual watershed SWE reconstructions have different end years, the earliest of which only extend to 1990. This implies that the similarity in patterns of anomalies are notable but that the magnitudes of departure should not be expected to be the same.

may have reduced runoff yield more than would be expected from estimated snowpack amounts alone. For example, average to slightly below-average snowpack prevailed from ~1118 to 1179 C.E. over most of the Upper Colorado basin, yet this was an extreme low-flow period in the streamflow reconstructions (fig. S4). This interval coincides with a period of elevated regional and hemispheric temperatures (*20*, *31*) that may have increased evapotranspiration and sublimation while decreasing soil- and shallow groundwater–recharge and storage. Warmer temperatures and severe decadal-scale snowpack reductions combined to produce an extreme low-flow interval during this period of the Medieval Climate Anomaly (~1143 to 1155 C.E.) (fig. S4). Such interactions between warmer temperatures and cool season precipitation have been documented for the hydrologic (water supply) droughts of the 1950s and early 2000s (*31*), which again raises concerns for the future of snow-temperature-runoff relationships throughout the North American cordillera.

Although the causes of synchronous winter snowpack declines are probably attributable to multiple factors in past centuries, the conspicuous breakdown of the N-S dipole after the 1980s (Figs. 1G, 3, and 4) may now reflect positive reinforcement of anthropogenic warming by decadal variability. Specifically, a decadal-scale shift in Pacific climate ~1976 to 1984 may account for nearly half (~30 to 50%) of the springtime warming in western North America, the trend in decreasing winter precipitation in the north and increasing winter precipitation in the south (*9*, *32*), and the more pronounced snowpack decline in the north. Hence, a decadal shift to cooling in the tropical and Northeast Pacific could temporarily mask the trend in springtime warming and declining snowpack.

Our reconstructions highlight the unusual nature of snowpack declines in northern watersheds and synchronous snowpack losses across the entire cordillera since the 1980s (Figs. 1G, 3, and 4). Together, these events may signal a fundamental shift from precipitation to temperature as the dominant influence on snowpack in the North American cordillera, with major consequences for regional water supplies (*2*, *10*).

References and Notes

1. R. C. Bales *et al.*, *Water Resour. Res.* **42**, W08432 (2006).
2. T. P. Barnett *et al.*, *Science* **319**, 1080 (2008).
3. M. G. Flanner, K. M. Shell, M. Barlage, D. K. Perovich, M. A. Tschudi, *Nat. Geosci.*; published online 16 January 2011 (2011.10.1038/ngeo1062).
4. G. T. Pederson *et al.*, *J. Clim.* **24**, 1666 (2010).
5. F. R. Hauer *et al.*, *Hydrol. Process.* **11**, 903 (1997).
6. J. S. Littell, D. McKenzie, D. L. Peterson, A. L. Westerling, *Ecol. Appl.* **19**, 1003 (2009).
7. M. D. Schwartz, *Glob. Change Biol.* **12**, 343 (2006).
8. A. L. Westerling, H. G. Hidalgo, D. R. Cayan, T. W. Swetnam, *Science* **313**, 940 (2006).
9. J. T. Abatzoglou, *Int. J. Climatol.*, published online 14 April 2010 (10.1002/joc.2137).
10. G. J. McCabe, D. M. Wolock, *Earth Interact.* **13**, 1 (2009).
11. P. W. Mote, *J. Clim.* **19**, 6209 (2006).
12. S. Solomon *et al.*, *Climate Change 2007: The Physical Science Basis. Contribution of Working Group I to the Fourth Assessment Report of the IPCC* (Cambridge Univ. Press, Cambridge, UK and New York, NY, USA, 2007).
13. P. C. D. Milly *et al.*, *Science* **319**, 573 (2008).
14. G. J. McCabe, J. L. Betancourt, S. T. Gray, M. A. Palecki, H. G. Hidalgo, *Quat. Int.* **188**, 31 (2008).
15. E. R. Cook, C. A. Woodhouse, C. M. Eakin, D. M. Meko, D. W. Stahle, *Science* **306**, 1015 (2004).
16. D. W. Stahle, F. K. Fye, E. R. Cook, R. D. Griffin, *Clim. Change* **83**, 133 (2007).
17. D. M. Meko *et al.*, *Geophys. Res. Lett.* **34**, L10705 (2007).
18. C. A. Woodhouse, S. T. Gray, D. M. Meko, *Water Resour. Res.* **42**, WO5415 (2006).
19. B. H. Luckman, R. J. S. Wilson, *Clim. Dyn.* **24**, 131 (2005).
20. M. W. Salzer, K. F. Kipfmuller, *Clim. Change* **70**, 465 (2005).
21. C. A. Woodhouse, *J. Clim.* **16**, 1551 (2003).
22. L. J. Graumlich, *Ann. Assoc. Am. Geogr.* **77**, 19 (1987).
23. D. W. Peterson, D. L. Peterson, *Ecology* **82**, 3330 (2001).
24. Materials and methods are available as supporting material on *Science* Online.
25. B. H. Luckman, *Geomorphology* **32**, 357 (2000).
26. T. Kitzberger, P. M. Brown, E. K. Heyerdahl, T. W. Swetnam, T. T. Veblen, *Proc. Natl. Acad. Sci. U.S.A.* **104**, 543 (2007).
27. M. D. Dettinger, D. R. Cayan, H. F. Diaz, D. M. Meko, *J. Clim.* **11**, 3095 (1998).
28. D. P. Brown, A. C. Comrie, *Geophys. Res. Lett.* **31**, L09203 (2004).
29. C. A. Woodhouse, J. L. Russell, E. R. Cook, *J. Clim.* **22**, 4336 (2009).
30. R. Wilson, G. Wiles, R. D'Arrigo, C. Zweck, *Clim. Dyn.* **28**, 425 (2007).
31. C. A. Woodhouse, D. M. Meko, G. M. MacDonald, D. W. Stahle, E. R. Cook, *Proc. Natl. Acad. Sci. U.S.A.* **107**, 21283 (2010).
32. T. R. Ault, A. K. Macalady, G. T. Pederson, J. L. Betancourt, M. D. Schwartz, *J. Clim.*, published online 11 February 2011 (10.1175/2011JCLI4069.1).

Acknowledgments: We thank S. Laursen for project assistance; G. McCabe and D. McWethey for helpful comments; and T. Chesley-Preston (USGS), L. Clampitt (USGS), S. Moore [Environmental Systems Research Institute (ESRI)], B. Ralston (ESRI), and L. Saunders (ESRI) for assistance building animations and Web-mapping tools for the snowpack database. We give a special thanks to contributors to the International Tree Ring Databank and M. Colenutt, D. Meko, and T. Knight for the invaluable tree-ring records. This research was financially supported in part by the USGS Western Mountain Initiative and NSF (grants GSS-0620793 and DEB-0734277). C.A.W. was supported by NSF (grants 980931 and 9729571), USGS Earth Surface Dynamics Program, and the Denver Water Board. J.S.L was supported by the Joint Institute for the Study of the Atmosphere and Ocean under National Oceanic and Atmospheric Administration (NOAA) Cooperative Agreement NA17RJ1232 (contribution 1856) and NOAA Climate Program Office Sector Applications Research Program (grant NA07OAR4310371). B.H.L was supported by the Natural Sciences and Engineering Research Council of Canada (grant 8847). Any use of trade, product, or firm names is for descriptive purposes only and does not imply endorsement by the U.S. government. G.T.P, S.T.G, C.A.W., and L.J.G planned the project, contributed data, and designed and participated in the data analyses and writing of the paper. G.T.P and S.T.G. conducted all the analyses. J.L.B. and D.B.F. contributed substantially to the analysis design and writing of the paper. J.S.L, E.W., and B.H.L provided critical northern cordilleran tree-ring chronologies and contributed to the writing of the paper. Reprints and permissions information is available online at www.sciencemag.org/site/about/permissions.xhtml. The authors declare no competing financial interests. All of the snowpack reconstructions and tree-ring chronologies used to generate them are available online at the World Data Center for Paleoclimatology in Boulder, Colorado, USA (www.ncdc.noaa.gov/paleo/pubs/pederson2011/pederson2011.html) and from the USGS Northern Rocky Mountain Science Center in Bozeman, Montana, USA (www.nrmsc.usgs.gov/NorthAmerSnowpack/).

Supporting Online Material

www.sciencemag.org/cgi/content/full/science.1201570/DC1
Materials and Methods
SOM Text
Figs. S1 to S4
Tables S1 to S6
References (*33*–*38*)

13 December 2010; accepted 20 May 2011
10.1126/science.1201570

Downloaded from www.sciencemag.org on July 18, 2011

www.sciencemag.org/cgi/content/full/science.1201570/DC1

Supporting Online Material for

The Unusual Nature of Recent Snowpack Declines in the North American Cordillera

Gregory T. Pederson,* Stephen T. Gray, Connie A. Woodhouse, Julio L. Betancourt, Daniel B. Fagre, Jeremy S. Littell, Emma Watson, Brian H. Luckman, Lisa J. Graumlich

*To whom correspondence should be addressed. E-mail: gpederson@usgs.gov

Published 9 June 2011 on *Science* Express
DOI: 10.1126/science.1201570

This PDF file includes:

Materials and Methods

SOM Text

Figs. S1 to S4

Tables S1 to S6

References (*33–38*)

Supporting Online Material for

The unusual nature of recent snowpack declines in the North American Cordillera

Authors:

[1,2,3]Gregory T. Pederson*, [3,4] Stephen T. Gray, [3,5]Connie A. Woodhouse, [6]Julio L. Betancourt, [1]Daniel B. Fagre, [7]Jeremy S. Littell, [8]Emma Watson, [9]Brian H. Luckman, and [10]Lisa J. Graumlich

Affiliations:

[1]U.S. Geological Survey, Northern Rocky Mountain Science Center, 2727 University Way (Suite 2), Bozeman, MT 59715; [2]School of Natural Resources, University of Arizona, 325 Biosciences East, Tucson, AZ 85721; [3]Laboratory of Tree-Ring Research, University of Arizona, 105 W. Stadium, Tucson, AZ 85721; [4]Department of Civil and Architectural Engineering, University of Wyoming, Laramie, WY 82071; [5]School of Geography and Development, 412 Harvill Building, University of Arizona, Tucson, Arizona 85721-0076; [6]U.S. Geological Survey, National Research Program, Water Resources Division, Tucson, AZ 85719; [7]Climate Impacts Group, University of Washington, Box 355672, Seattle, WA 98195-5672; [8]Aurora, Ontario, Canada; [9]Department of Geography, University of Western Ontario, London, Ontario, Canada N6A 5C2; [10]College of the Environment, University of Washington, Box 355679, Seattle, WA 98195-5679

***To whom correspondence should be addressed:** gpederson@usgs.gov

Materials and Methods

Methods Summary

We generated snowpack reconstructions for each basin using a spatially- and temporally-nested stepwise regression strategy similar to that employed to reconstruct river flows (*17, 18*). Briefly, reconstructions were first attempted using a "basin limited" approach that included only those chronologies located within 50 km of each watershed. If target levels for skill and validation (*17, 18*) were not obtained, the search area was increased to the sub-region (e.g., Greater Yellowstone), and finally to a pool of all available tree-ring chronologies. Once a snowpack model was obtained that optimized variance explained, subsequent nested regression procedures were used to generate successively longer reconstructions, albeit with diminished skill, using subsets of predictor chronologies filtered by their start year. To remove potential artifacts caused by the nesting of successively longer reconstructions, means and variances were scaled to match the first skill-optimized reconstruction. Records were then combined into a single continuous, long-duration snowpack reconstruction for each watershed. This process was repeated for each watershed, resulting in a total of 128 models that integrate information from 66 chronologies (Tables S2 - S5). A comparison of the final 27 composite watershed-level snowpack reconstructions against observed April 1 SWE shows that the models skillfully capture both interannual and decadal variability, and can provide detailed estimates of long-term snowpack history (Fig. S1).

Tree-ring data and standardization

All potential predictor chronologies used in the snowpack reconstructions are from recent collections of the co-authors and/or a subset of records contributed to the World Data Center for Paleoclimatology's International Tree-Ring Data Bank (ITRDB, http://www.ncdc.noaa.gov/paleo/treering.html). Radial growth artifacts were removed from all individual tree records using conservative detrending methods (negative exponential or straight line fit). These individual records were combined into site chronologies using a robust weighted mean and variance-stabilization to account for possible trends in variance due to changing numbers of samples through time (*17, 18, 33*). Standard (i.e., serial autocorrelation retained) and pre-whitened (autocorrelation removed) versions of the chronologies were produced for each site. However, only those analyses based on standard chronologies are presented herein, as the observational records contained serial persistence.

Watershed-level snowpack datasets

Though exceptions occur, SWE measurements made on April 1 generally represent a robust estimate of the annual peak accumulation of snowpack in the NA cordillera (*1, 4, 11, 34*), and in conjunction with automated daily SWE measurements, inform seasonal streamflow forecasting and water resource management and planning. Consequently our analyses focus on April 1 SWE values. The accurate measurement of SWE at any single point is, however, exceedingly difficult; once on the ground, snowpack changes continuously in response to wind and fluxes of energy and moisture, all of which are related to atmospheric pressure and circulation (*1*). In turn, interactions between synoptic drivers and local conditions introduce a substantial amount of finer-

scale variability into point measurements of snow. As a result, we aggregated individual site observations up to the level of watersheds, thereby lessening the impact of the local environment, as well as measurement and equipment-related error. Our own analyses and prior work (*4*), and the work of others (e.g. *2*) show that this approach provides the best approximation for a common regional peak-snowpack signal. The U.S. Natural Resources Conservation Service (NRCS; http://www.wcc.nrcs.usda.gov/snowcourse/) first began manual measurements of SWE in the 1920s with comprehensive coverage attained by ~1950, and the observational records used in this study span these same periods. Accordingly, the range of dates over which April 1 SWE measurements are available varies from watershed to watershed, making the window over which tree-ring screening and model calibrations were performed variable. Generally, most all models were calibrated over a time interval spanning 1936 to 1990, though some continued into the early 2000s depending on the end date of the most limiting chronology. All calibration intervals and associated degrees of freedom for specific watershed reconstructions can be found in tables S5.1 – S5.4.

Chronology screening and growth-climate relationships

Tree-ring chronologies from the ITRDB were screened to ensure they were not collected for use in ecological or fire history studies, and that they ended in at least 1980. All chronologies were screened for significant ($p \leq 0.05$) relationships with watershed-level April 1 SWE at year t and $t \pm 1$. There were few cases of significant lag/lead correlations, so only growth at year t was included in subsequent modeling. With few exceptions, models extended to and beyond the 1990s. This ensured the tree-ring chronologies accurately captured events in recent decades, and therefore provide a robust means for comparing observational records against patterns of long-term variability. Additionally, the network of winter snowpack sensitive trees contains both low-elevation and high-elevation tree species that exhibit positive and negative growth responses, respectively. This strategy results in models that are rougly equivalent in their ability to capture extreme high- and low-snowpack years.

Snowpack model construction

The nested, multiple linear regression models of April 1 SWE were constructed using a forward-backward stepwise regression procedure that allowed screened predictor chronologies to enter at $\alpha = 0.05$, with a removal $\alpha = 0.10$ (*18*). Model strength was summarized using adjusted R^2 and F level, and potential problems with multicolinearity of predictors examined using the variance inflation factor (VIF) statistic. To prevent model overfitting, the entry of predictors was halted when it resulted in either an increase in root mean squared error ($RMSE_v$) or a decrease in validation R^2 (also known as reduction of error, or RE) statistic. Model validation was conducted using a leave-one-out cross-validation procedure (i.e., PRESS). The use of PRESS was chosen over data subsetting into different calibration and validation intervals because of the relatively short length of the April 1 SWE records. We also developed reconstructions for larger watersheds and regions using stepwise regression (Tables S5.2 and S5.4). Principal components analysis (PCA) based regressions (not shown) were used as a quality check on the SWE reconstructions. The reconstructions cross-validated well (Table S5.1-S5.4) with the occasional exception of the Durban-Watson (DW) statistic indicating the

potential for problems with autocorrelation in the residuals. Visual inspection of the residual plots and additional sensitivity tests showed these problems to be minor and typically driven by a series of years in the early portion of the observed SWE record. More specific information on the methodologies employed here can be found in Woodhouse et al. (*18*) and Meko et al. (*17*).

Data Access

All snowpack reconstructions and tree-ring chronologies used to generate them are available online at the World Data Center for Paleoclimatology in Boulder, Colorado, U.S.A. (http://www.ncdc.noaa.gov/paleo/pubs/pederson2011/pederson2011.html), and from the U.S. Geological Survey Northern Rocky Mountain Science Center in Bozeman, Montana, U.S.A. (http://www.nrmsc.usgs.gov/NorthAmerSnowpack/). High-resolution versions of the supplemental figures and a web-mapping tool that allows for the generation of user-defined snowpack anomaly maps and animations are also available from the USGS website.

Supporting Online Text

Modes of Variability in Snowpack

The dominant frequencies of snowpack variability are assessed in a wavelet analysis on the regional SWE averages calculated from individual watersheds (i.e. HUC6) (Fig. S2). The wavelet analyses were performed using a morlet wavelet with a scale-width resolution of 0.2 and significance testing performed against a red-noise (AR1) background (*35, 36*). Results show significant low-frequency (16 to 80+ years) variability is a defining feature of snowpack within the NA cordillera - with relatively temporally stable and strong inter-decadal (20-80 year) persistence (Fig. S2). The northern watersheds exhibit significant centennial-scale variability that is largely absent across the Upper Colorado region. Power increases in the centennial-scale frequencies over the late-19th and 20th centuries due to recent and rapid snowpack declines across the northern watersheds, though most of this falls within the cone of influence. The Upper Colorado exhibits greater interannual variability (2-8 year) than the northern watersheds throughout the length of record. Interannual variability across the northern watersheds is weak throughout the length of record, with few significant events appearing during the sustained high snowpack conditions of the LIA (~1700 -1900).

North-south snowpack dipole analysis

An assessment of the N-S snowpack dipole shown in Fig. S3 was performed using PCA (varimax rotated and unrotated, not shown) on the correlation matrix of the individual HUC 6 watershed April 1 SWE reconstructions over a common interval (1500-1990). Results support our interpretation of Fig. 3, splitting the southern and northern cordilleran watersheds onto the first and second components respectively, explaining 54% of the total variance, with time-series plots of the component scores showing stationarity in the N-S snowpack dipole. An additional 14.6% of the variance is explained by the third principal component, which indicates the northern watersheds of the Upper Colorado region (i.e., the Webber, Green, White-Yampa, and the North and South Platte) contain variance orthogonal to both the northern or southern cordillera. The variance of the individual watershed reconstructions, and the time-series plot of the component scores, suggest these watersheds in particular are a dynamic boundary between the N-S dipole. For example, at the height of the LIA these watersheds mirror average snowpack conditions in the northern cordillera (Fig. 2e), whereas during the 1450s and 1550s drought (Fig 2a,c) conditions are more similar to those shown across the southern cordillera.

Supplementary Figures

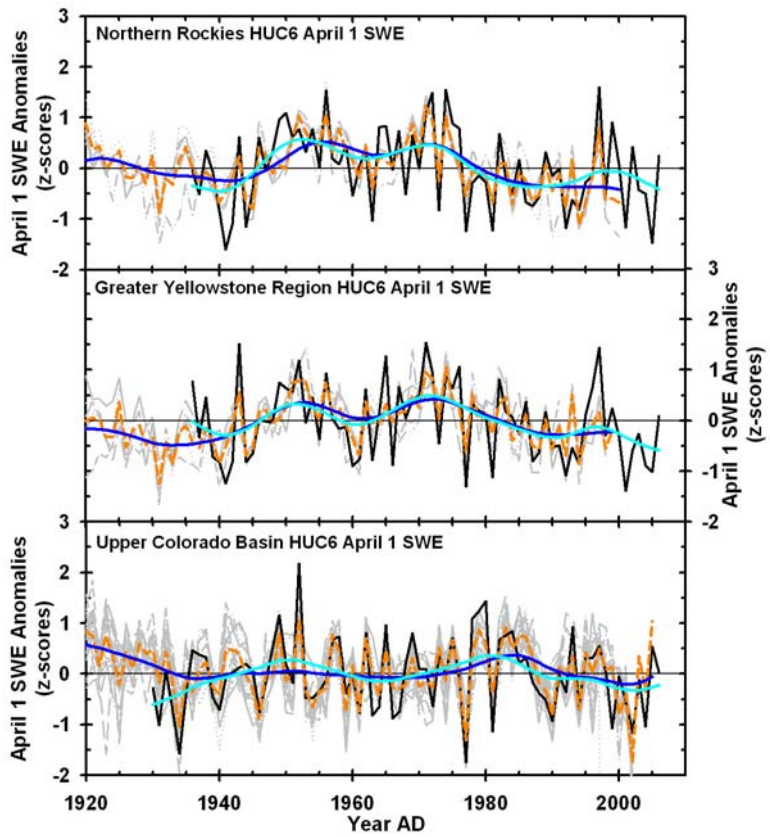

Figure S1. Watershed-based observed and reconstructed April 1 SWE. Observed April 1 SWE regional averages (black lines) were calculated from individual snow course records, and plotted alongside the tree-ring based HUC6 watershed SWE reconstructions (gray lines) and the reconstructed regional average SWE conditions (dashed orange lines). Both the observed (cyan line) and reconstructed regional averages of (dark blue line) April 1 SWE are shown smoothed with a 20-year cubic-smoothing spline (50% frequency cutoff) to highlight correspondence at decadal-scales. Note the spline is biased by end effects at the start and end of any time series, and this bias is particularly evident at the start of the observed April 1 SWE records (~1920 to 1930 AD).

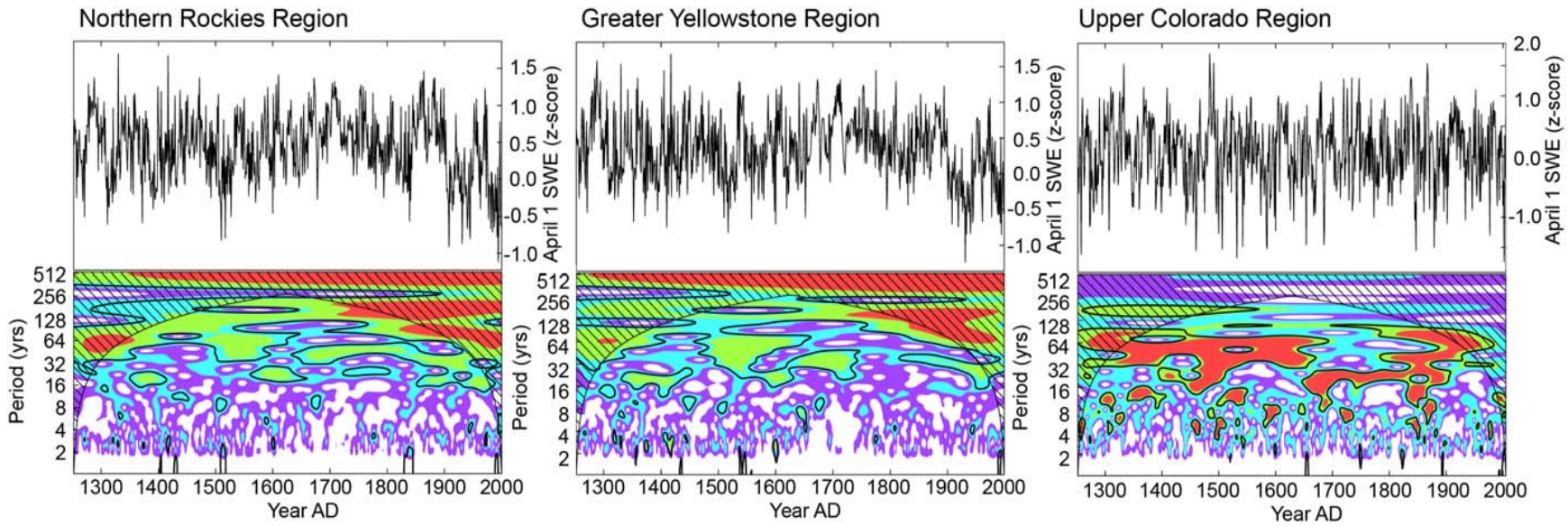

Figure S2. Wavelet analysis of regional April 1 SWE averages. (Top) Regional April 1 SWE averages calculated from individual HUC6 watershed reconstructions. (Bottom) The wavelet power spectrum. Contour levels are chosen so that 0%, 25% 50%, 75%, and >90% of the wavelet power is above each level, and represented with white, purple, blue, green, and red respectively. The cross-hatched region is the cone of influence, where zero padding has reduced the variance. Black contour is the 90% significance level, using a red-noise (AR1) background spectrum. Analysis performed in (*35*) with methods based on (*36*).

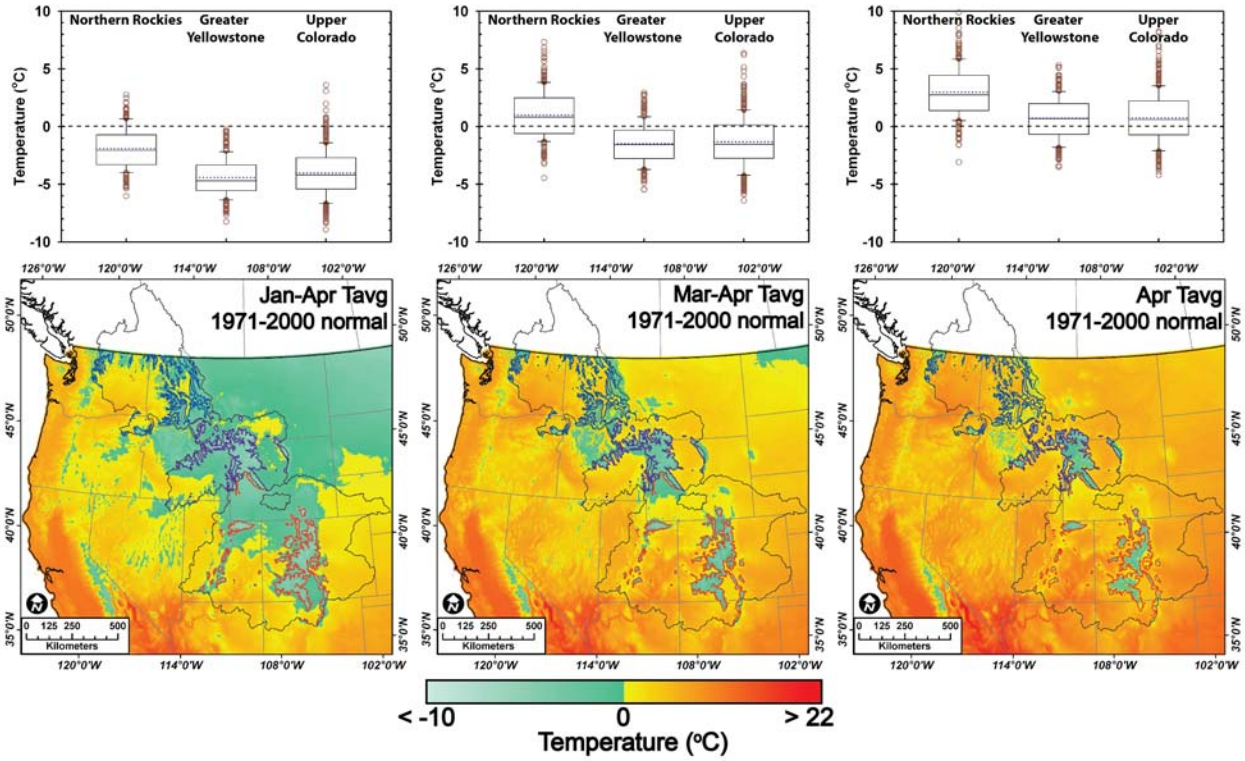

Figure S3. Average seasonal and monthly temperatures of snow dominated landmasses (below) and snow course measurement sites (above) across the three study regions for critical winter and spring snow accumulation months. Average temperatures were calculated, mapped, and estimated at each snow course site using PRISM (37, 38) (http://www.prism.oregonstate.edu/) 800m 1971-2000 climate normals, and the distribution of average temperatures is shown for each region using a box and whisker plot. The average elevation of snow course monitoring sites for each of the three regions is shown with a different color contour line.

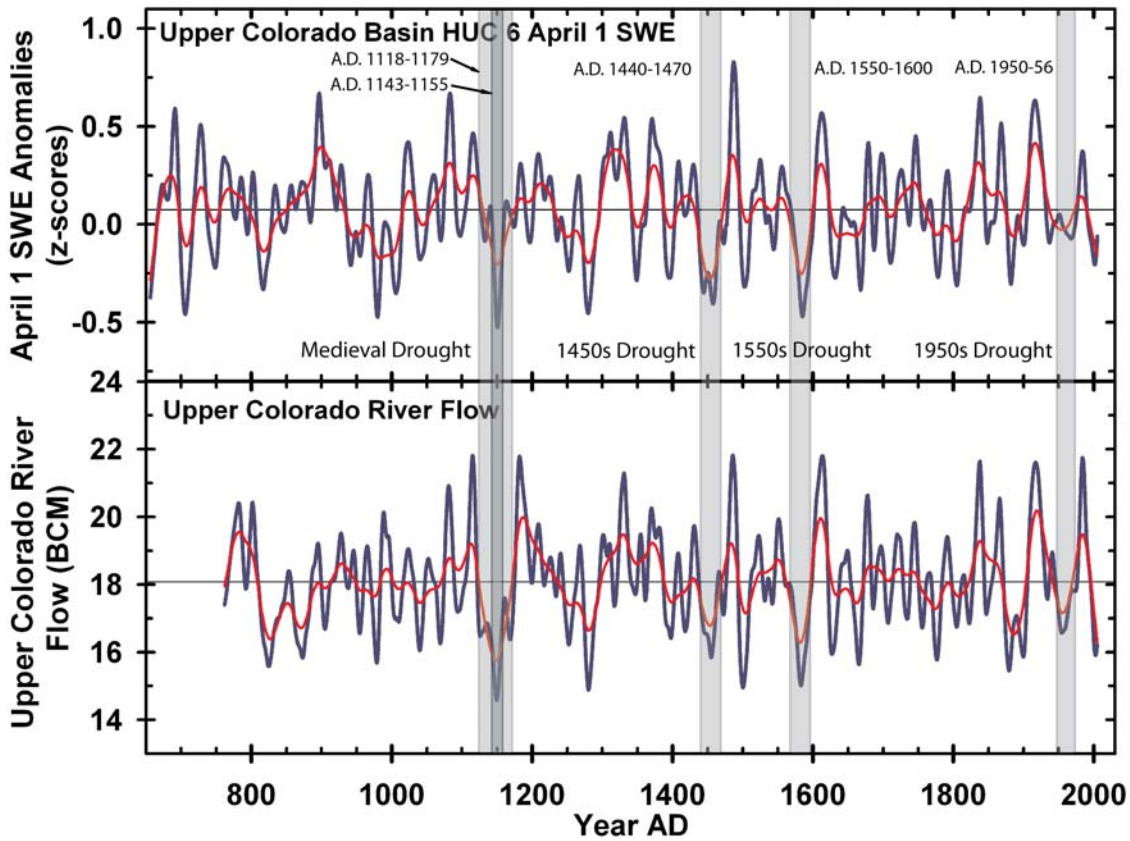

Figure S4. Comparison of decadal-scale variability in estimates of Upper Colorado Basin April 1 SWE and total annual streamflow. For clarity, each reconstruction is shown with a 20-year (dark blue line) and 50-year (red line) cubic-smoothing spline (50% frequency cutoff), shown as departures from the long-term mean. The discussed low flow periods are highlighted with gray bars. The reconstructed Upper Colorado River flows (*17*) are plotted in billions of cubic meters (BCM), and were calibrated against the Lee's Ferry gauge record.

Supplementary Tables

Table S1. Summary of snow course April 1 SWE sampling site elevations by region.

Region	No.	Mean ele. (m)	Median ele. (m)	Max ele. (m)	Min ele. (m)	σ (m)
Northern Rockies	373	1544	1532	2516	345	424
Greater Yellowstone	279	2307	2288	3093	1708	291
Upper Colorado	305	2807	2837	3538	1678	311

Table S2. Summary of April 1 SWE models by region.

Regions	# Models	# Chronologies
Northern Rockies and Greater Yellowstone (HUC6)	38	28
Northern Rockies and Greater Yellowstone (Large Watersheds)	12	13
Upper Colorado (HUC6)	52	34
Upper Colorado (Large Watershed)	26	22
Total:	128	66*

*Total number of chronologies used in all models. Replicate appearances by individual chronologies have been removed.

Table S3. List of tree-ring chronologies that entered one or more of the 128 nested April 1 SWE regression models. Tables also available at: http://www.nrmsc.usgs.gov/NorthAmerSnowpack/data/ and http://www.ncdc.noaa.gov/paleo/pubs/pederson2011/pederson2011.html.

Table S4. Tree-ring chronologies (standard version) that entered one or more of the 128 nested April 1 SWE regression models. Tables also available at: http://www.nrmsc.usgs.gov/NorthAmerSnowpack/data/ and http://www.ncdc.noaa.gov/paleo/pubs/pederson2011/pederson2011.html.

Table S5.1 – S5.4. April 1 SWE nested model calibration and validation statistics. The "MV adjust" and "In composite" columns indicate whether a particular reconstruction had it's mean and variance scaled to match the mean and variance (calculated over a common interval) of the "best" SWE reconstruction before inclusion into the composite reconstruction of snowpack. If the mean and variance was not adjusted, it was not included in the composite record due to model issues. Tables also available at: http://www.nrmsc.usgs.gov/NorthAmerSnowpack/data/ and http://www.ncdc.noaa.gov/paleo/pubs/pederson2011/pederson2011.html.

Table S6. Different long-term April 1 SWE averages calculated using three different base periods.

Region	**1400-1950 (z-scores)**	**1400-Present (z-scores)**	**Full Record (z-scores)**
Northern Rocky Mountains	0.463	0.431	0.432
Greater Yellowstone	0.369	0.346	0.350
Upper Colorado	0.074	0.070	0.076

References and Notes

1. R. C. Bales *et al*., Mountain hydrology of the western United States. *Water Resour. Res.* **42**, W08432 (2006). doi:10.1029/2005WR004387

2. T. P. Barnett *et al*., Human-induced changes in the hydrology of the western United States. *Science* **319**, 1080 (2008). doi:10.1126/science.1152538 Medline

3. M. G. Flanner, K. M. Shell, M. Barlage, D. K. Perovich, M. A. Tschudi, *Nat. Geosci.* Published online 16 January 2011. 10.1038/ngeo1062

4. G. T. Pederson *et al*., Climatic Controls on the Snowmelt Hydrology of the Northern Rocky Mountains. *J. Clim.* **24**, 1666 (2010). doi:10.1175/2010JCLI3729.1

5. F. R. Hauer *et al*., ASSESSMENT OF CLIMATE CHANGE AND FRESHWATER ECOSYSTEMS OF THE ROCKY MOUNTAINS, USA AND CANADA. *Hydrol. Process.* **11**, 903 (1997). doi:10.1002/(SICI)1099-1085(19970630)11:8<903::AID-HYP511>3.0.CO;2-7

6. J. S. Littell, D. McKenzie, D. L. Peterson, A. L. Westerling, Climate and wildfire area burned in western U.S. ecoprovinces, 1916-2003. *Ecol. Appl.* **19**, 1003 (2009). doi:10.1890/07-1183.1 Medline

7. M. D. Schwartz, R. AHAS, A. AASA. *Glob. Change Biol.* **12**, 343 (2006). doi:10.1111/j.1365-2486.2005.01097.x

8. A. L. Westerling, H. G. Hidalgo, D. R. Cayan, T. W. Swetnam, Warming and earlier spring increase western U.S. forest wildfire activity. *Science* **313**, 940 (2006). doi:10.1126/science.1128834 Medline

9. J. T. Abatzoglou, *Int. J. Climatol.* Published online 14 April 2010. 10.1002/joc.2137

10. G. J. McCabe, D. M. Wolock, Recent Declines in Western U.S. Snowpack in the Context of Twentieth-Century Climate Variability. *Earth Interact.* **13**, 1 (2009). doi:10.1175/2009EI283.1

11. P. W. Mote, Climate-Driven Variability and Trends in Mountain Snowpack in Western North America. *J. Clim.* **19**, 6209 (2006). doi:10.1175/JCLI3971.1

12. S. Solomon *et al*., *Climate Change 2007: The Physical Science Basis. Contribution of Working Group I to the Fourth Assessment Report of the IPCC*. (Cambridge University Press, Cambridge, United Kingdom and New York, NY, USA, 2007), pp. 996.

13. P. C. D. Milly *et al*., Climate change. Stationarity is dead: whither water management? *Science* **319**, 573 (2008). doi:10.1126/science.1151915 Medline

14. G. J. McCabe, J. L. Betancourt, S. T. Gray, M. A. Palecki, H. G. Hidalgo, Associations of multi-decadal sea-surface temperature variability with US drought. *Quat. Int.* **188**, 31 (2008). doi:10.1016/j.quaint.2007.07.001

15. E. R. Cook, C. A. Woodhouse, C. M. Eakin, D. M. Meko, D. W. Stahle, Long-term aridity changes in the western United States. *Science* **306**, 1015 (2004). doi:10.1126/science.1102586 Medline

16. D. W. Stahle, F. K. Fye, E. R. Cook, R. D. Griffin, Tree-ring reconstructed megadroughts over North America since a.d. 1300. *Clim. Change* **83**, 133 (2007). doi:10.1007/s10584-006-9171-x

17. D. M. Meko *et al*., Medieval drought in the upper Colorado River Basin. *Geophys. Res. Lett.* **34**, L10705 (2007). doi:10.1029/2007GL029988

18. C. A. Woodhouse, S. T. Gray, D. M. Meko, Updated streamflow reconstructions for the Upper Colorado River Basin. *Water Resour. Res.* **42**, WO5415 (2006). doi:10.1029/2005WR004455

19. B. H. Luckman, R. J. S. Wilson, Summer temperatures in the Canadian Rockies during the last millennium: a revised record. *Clim. Dyn.* **24**, 131 (2005). doi:10.1007/s00382-004-0511-0

20. M. W. Salzer, K. F. Kipfmuller, Reconstructed Temperature And Precipitation On A Millennial Timescale From Tree-Rings In The Southern Colorado Plateau, U.S.A. *Clim. Change* **70**, 465 (2005). doi:10.1007/s10584-005-5922-3

21. C. A. Woodhouse, A 431-Yr Reconstruction of Western Colorado Snowpack from Tree Rings. *J. Clim.* **16**, 1551 (2003). doi:10.1175/1520-0442-16.10.1551

22. L. J. Graumlich, Precipitation Variation in the Pacific Northwest (1675-1975) as Reconstructed from Tree Rings. *Ann. Assoc. Am. Geogr.* **77**, 19 (1987). doi:10.1111/j.1467-8306.1987.tb00142.x

23. D. W. Peterson, D. L. Peterson, MOUNTAIN HEMLOCK GROWTH RESPONDS TO CLIMATIC VARIABILITY AT ANNUAL AND DECADAL TIME SCALES. *Ecology* **82**, 3330 (2001). doi:10.1890/0012-9658(2001)082[3330:MHGRTC]2.0.CO;2

24. Materials and methods are available as supporting material on *Science* Online.

25. B. H. Luckman, The Little Ice Age in the Canadian Rockies. *Geomorphology* **32**, 357 (2000). doi:10.1016/S0169-555X(99)00104-X

26. T. Kitzberger, P. M. Brown, E. K. Heyerdahl, T. W. Swetnam, T. T. Veblen, Contingent Pacific-Atlantic Ocean influence on multicentury wildfire synchrony over western North America. *Proc. Natl. Acad. Sci. U.S.A.* **104**, 543 (2007). doi:10.1073/pnas.0606078104 Medline

27. M. D. Dettinger, D. R. Cayan, H. F. Diaz, D. M. Meko, North–South Precipitation Patterns in Western North America on Interannual-to-Decadal Timescales. *J. Clim.* **11**, 3095 (1998). doi:10.1175/1520-0442(1998)011<3095:NSPPIW>2.0.CO;2

28. D. P. Brown, A. C. Comrie, *Geophys. Res. Lett.* **31**, ▪▪▪ (2004).

29. C. A. Woodhouse, J. L. Russell, E. R. Cook, Two Modes of North American Drought from Instrumental and Paleoclimatic Data. *J. Clim.* **22**, 4336 (2009). doi:10.1175/2009JCLI2705.1

30. R. Wilson, G. Wiles, R. D'Arrigo, C. Zweck, Cycles and shifts: 1,300 years of multi-decadal temperature variability in the Gulf of Alaska. *Clim. Dyn.* **28**, 425 (2007). doi:10.1007/s00382-006-0194-9

31. C. A. Woodhouse, D. M. Meko, G. M. MacDonald, D. W. Stahle, E. R. Cook, A 1,200-year perspective of 21st century drought in southwestern North America. *Proc. Natl. Acad. Sci. U.S.A.* **107**, 21283 (2010). doi:10.1073/pnas.0911197107 Medline

32. T. R. Ault, A. K. Macalady, G. T. Pederson, J. L. Betancourt, M. D. Schwartz, *J. Clim.* Published online 11 February 2011. 10.1175/2011JCLI4069.1

33. E. R. Cook, K. Briffa, S. Shiyatov, V. Mazepa, in *Methods of Dendrochonology: Applications in the Environmental Sciences,* E. R. Cook, L. A. Kairiukstis, Eds. (Springer, New York, 1990), pp. 104-123.

34. G. S. Bohr, E. Aguado, Use of April 1 SWE measurements as estimates of peak seasonal snowpack and total cold-season precipitation. *Water Resour. Res.* **37**, 51 (2001). doi:10.1029/2000WR900256

35. A. G. Bunn, A dendrochronology program library in R (dplR). *Dendrochronologia* **26**, 115 (2008). doi:10.1016/j.dendro.2008.01.002

36. C. Torrence, G. P. Compo, A Practical Guide to Wavelet Analysis. *Bull. Am. Meteorol. Soc.* **79**, 61 (1998). doi:10.1175/1520-0477(1998)079<0061:APGTWA>2.0.CO;2

37. C. Daly, W. P. Gibson, G. H. Taylor, G. L. Johnson, P. Pasteris, A knowledge-based approach to the statistical mapping of climate. *Clim. Res.* **22**, 99 (2002). doi:10.3354/cr022099

38. C. Daly *et al*., Physiographically sensitive mapping of climatological temperature and precipitation across the conterminous United States. *Int. J. Climatol.* **28**, 2031 (2008). doi:10.1002/joc.1688

Acknowledgments: We thank S. Laursen for project assistance, G. McCabe and D. McWethey for helpful comments, and T. Chesley-Preston (USGS), L. Clampitt (USGS), and S. Moore, B. Ralston, and L. Saunders of ESRI for assistance building animations and web-mapping tools for the snowpack database. A special thanks to contributors to the International Tree Ring Databank, M. Colenutt, D. Meko, and T. Knight for the invaluable tree-ring records. This research was financially supported in part by the USGS Western Mountain Initiative, and the NSF (grants GSS-0620793 and DEB-0734277). C.A.W. was supported by NSF (grants 980931 and 9729571), USGS Earth Surface Dynamics Program, and the Denver Water Board. J.S.L was supported by the Joint Institute for the Study of the Atmosphere and Ocean (JISAO) under NOAA Cooperative Agreement NA17RJ1232 (contribution 1856), and NOAA Climate Program Office Sector Applications Research Program (grant NA07OAR4310371). B.H.L was supported by the Natural Sciences and Engineering Research Council of Canada (grant 8847). Any use of trade, product, or firm names is for descriptive purposes only and does not imply endorsement by the U.S. Government. G.T.P, S.T.G, C.A.W., and L.J.G planned the project, contributed data, designed and participated in the data analyses and writing of the paper. G.T.P and S.T.G. conducted all the analyses. J.L.B. and D.B.F. contributed substantially to the analysis design and writing of the paper. J.S.L, E.W., and B.H.L provided critical northern cordilleran tree-ring chronologies and contributed to the writing of the paper. Reprints and permissions information is available online at www.sciencemag.org/site/about/permissions.xhtml. The authors declare no competing financial interests. Correspondence and requests for materials should be addressed to

G.T.P. All the snowpack reconstructions, and tree-ring chronologies used to generate them, are available online at the World Data Center for Paleoclimatology in Boulder, Colorado, U.S.A. (http://www.ncdc.noaa.gov/paleo/pubs/pederson2011/pederson2011.html), and from the U.S. Geological Survey Northern Rocky Mountain Science Center in Bozeman, Montana, U.S.A. (http://www.nrmsc.usgs.gov/NorthAmerSnowpack/).